33rd Annual International Conference of the IEEE EMBS
Boston, Massachusetts USA, August 30 - September 3, 2011

3D Imaging for Quantitative Assessment of Toxicity on Vascular Development in Zebrafish

Charu Hans, Amol Shete, Shishir K. Shah, *Senior Member, IEEE*, Catherine W. McCollum, Maria B Bondesson, and Fatima A. Merchant, *Senior Member, IEEE*

***Abstract*— In this study, we describe the utility of the zebrafish model of in-vivo blood vessel formation as a tool for chemical risk assessment. Time-lapse confocal imaging of embryonic vasculature in the zebrafish is used in conjunction with digital image analysis to monitor and quantify the effect of toxins on vascular development. Non-rigid registration is used to capture changes in vascular morphology over time. Vascular formation in healthy normal and arsenic treated embryos was evaluated for differences in vascular structure using the algorithms developed. Although, the temporal progression of vascular development was similar, significant differences were observed in vessel structure between the toxin treated and healthy fish. This study revealed, for the first time, that vital vascular structures in fish maybe affected by exposure to arsenic. This technique allowed visualization of vascular abnormalities in embryos showing no external signs of malformations.**

I. INTRODUCTION

Zebrafish is an excellent model for studying vasculature development and human disease, largely because of its small size, transparency, easy availability, and external fertilization. More specifically, numerous studies have been reported in recent years involving the use of zebrafish to study effects of toxicity on vasculature development [16], [17]. Advantages of the zebrafish as a model for human diseases and drug discovery, together with differences with other animal models, have been extensively reviewed [2], [3].

The vascular system is a vital component of all vertebrate animals, supplying oxygen and essential nutrients to every tissue and organ. Early stages of embryonic development are particularly susceptible to adverse effects of chemicals. Unfortunately, these stages are the most inaccessible in the traditional mammalian models of toxicology. A wide range of congenital diseases are associated with blood vessel formation [1], development of the cardiovascular system and associated vascular defects [6]–[9], and the adverse effects of exposure to toxic elements during early development. Being able to model the growth of blood vessel in the vascular system is both interesting for understanding of vasculature system in humans, and for understanding the influence of various chemicals on vascular development.

Toxic materials, such as arsenic are associated with a multitude of human health problems; however, their impact on vasculature system has not been extensively studied. Inorganic form of arsenic is considered to be toxic and this pollutant is posing danger to humans by intake of affected fish, ground water exposed to toxins, etc. Zebrafish has proven to be excellent model to study toxic effects at the molecular level [11], [12], but its utility to study vascular growth is still unclear.

In this work, we use a transgenic zebrafish that expresses green fluorescent protein (GFP) in the vascular system Tg(Flk1:GFP) [18] to visualize vessel growth in the fish embryo. This transgenic zebrafish line expresses GFP in vascular endothelial cells, which permits real-time imaging of the formation and growth of blood vessels. Imaging captures the dynamics of blood vessel formation over time. In order to quantify these morphological changes, i.e. how much vascular structure has changed over a period of time, it is necessary to compensate for any movements caused by the growing embryo. Thus, in order to record the temporal changes occurring due to vessel growth, it is necessary to establish spatial correspondence between blood vessels that may appear displaced due to embryo movement. Thus quantitation of temporal vascular growth can be seen as a problem of image registration. The goal of image registration is to align two images, so that common features overlap and differences are emphasized. Image registration has been used widely in the medical field to quantify the influence of changes over time. As an example, registration is required in medicine for comparing computer tomography (CT) of patients scan [14], aligning images from various different modalities to diagnose diseases, etc. Recently, image registration has found application in growth monitoring of tumors and bone [10], [13].

In this paper, we use a non–rigid registration approach to align images. Non-rigid mapping is based on complete correspondence of images and includes a deformation model as the underlying transformation. We utilize free-

Manuscript received April 15, 2011.

C. Hans is with the Department of Computer Science, University of Houston, Houston, TX 77204 USA (e-mail: charuhans85@gmail.com).

A. Shete is with the Department of Computer Science, University of Houston, Houston, TX 77204 USA (e-mail: amol.shete1984@gmail.com).

S. K. Shah is with the Department of Computer Science, University of Houston, Houston, TX 77204 USA (e-mail: sshah@central.uh.edu).

C. McCollum is with the Department of Biology and Biochemsitry, University of Houston, Houston, TX 77204 USA (e-mail: mailto:cwmccoll@central.uh.edu).

M. Bondesson is with the Department of Biology and Biochemistry, University of Houston, Houston, TX 77204 (e-mail: ebondess@central.uh.edu).

F. A. Merchant is with the Department of Engineering Technology, University of Houston, Houston, TX 77204 USA (phone: 713-743-8292; fax: 713-743-0172; e-mail: fmerchant@uh.edu).

form deformation based on B-splines for growth monitoring, and use intensity differences as a similarity measure.

In Section II, we describe specimen preparation and data acquisition. We also present the approach for non–rigid registration and quantification of vascular growth. Section III discusses the experimental details and results, followed by conclusion and future work in section IV.

II. MATERIALS AND METHODS

A. Specimen Preparation

Adult transgenic zebrafish Tg(Flk1:GFP) were maintained and spawned as described in [15]. They were maintained at 28°C on a 14-h light and 10-h dark cycle. Tg(Flk1:GFP) embryos were collected during the first hour after fertilization and incubated in E3 medium (5mM NaCl, 0.17mM KCl, 0.33mM CaCl2, 0.33mM MgSO4, 0.00001% (w/v) Methylene Blue). Normally developing embryos were selected at 4- to 16-cell stage for subsequent arsenite treatments under a stereomicroscope (Leica MZ6).

For time lapse-imaging, Tg(Flk1:GFP) embryos at approximately 18-20 hpf were first selected for positive GFP expression under a fluorescent microscope (Olympus IX51 or Nikon AZ100M), then manually dechorionated and anesthetized with MS-222 (Tricaine). Subsequently, the

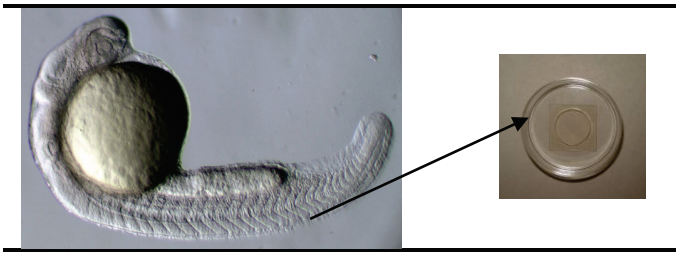

Fig 1. (a) The embryo is mounted in a glass bottom petri-dish using 1-2% agarose. The dish is placed bottom side up on an upright microscope stage. (b) The embryo is focused until GFP expression in the dorsal aorta is observed and imaging parameters such as the depth to be imaged, fluorophore and filter settings, laser power and offset, and mode of imaging (line or frame) are determined and set.

embryos were mounted in 0.3% (w/v) low-gelling agarose (Sigma-Aldrich cat. # A9045) in a glass-bottom culture dish (MatTek cat. #P35G-0-10-C). 0.003% (w/v) PTU and 0.03% (w/v) MS-222 were added to the mounting medium to prevent pigment expression and movement, respectively. Embryos were positioned on their sides in a thin layer of low-gelling agarose medium on the glass surface as shown in figure 1. Before the mounting medium reaches polymerization completely, more low-gelling agarose medium was added to form a mound. After the mounting medium has completely polymerized, E3-0.003% PTU media was added to the rim of the culture dish to prevent any air bubbles or pockets. 8-10 drops of 0.4% (w/v) MS-222 was also added to the culture dish. A strip of parafilm was used to secure the lid to the culture dish.

B. Chemical Dosage

Tg(Flk1:GFP) embryos were exposed to 400ug/mL of sodium arsenite (Sigma-Aldrich cat. #71287) starting at approximately 1 hour post fertilization (hpf). Control healthy embryos were treated in E3 medium only. Additionally, 0.003% (w/v) 1-phenyl-2-thiourea (PTU; Sigma-Aldrich cat. #P7629) was added to each well on Day 2 to suppress pigment expression [15].

C. Data Acquisition

Confocal image stacks were obtained using an Olympus Fluoview System. Vascular structure was imaged for a period of 16.5 – 24 hours after sample preparation. Scanning time was 2 minutes and rest time between two stacks was 15 minutes. Approximately 50 – 100 z-stacks were captured using 20X objective lens. Images were generated in TIFF format with 8-bit intensity depth. Image size was 512 pixels by 512 pixels. Maximum intensity projection (MIP) was computed for stack of images. MIP algorithm selects the brightest voxel along the z-axis and projects it on the orthogonal image plane. Figure 2 shows MIP's for unexposed and exposed embryo.

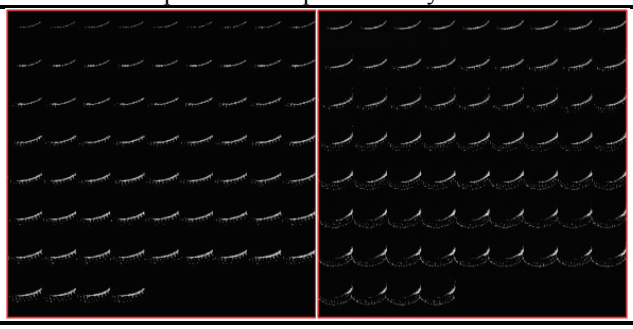

Fig 2. (a) Vascular development for unexposed embryo. (b) Vascular development for arsenic exposed embryo.

D. Image Registration

The goal of image registration is to find an optimum mapping that aligns two images. Since deformations are important for quantification of changes in images, it is necessary to find a mapping between two time points as accurately as possible. In our case we need to quantify blood vessel growth independent of motion artifacts. Hence we need a registration approach that establishes vessel correspondence between successive time frames. Affine and rigid registration approaches are mainly based on local stretching of images, and hence do not adequately capture structural changes.

Many applications in medicine require that object is modified in global scale. Therefore, we have used free-form deformation (FFD). Free form deformation deforms an object by warping the image geometry in which the object is localized. The nature of deformation varies widely across different time points; hence it is difficult to use traditional B-spline registration, which is based on many parameters. If we only select few parameters, an approximate match can be obtained, whereas many parameters incur added

computational costs. Hence, we have used FFD based on hierarchical B-splines for multilevel nonlinear registration [5]. The underlying idea of FFD is based on deforming an object by manipulating a mesh of 2D points.

Let $\Omega = \{(x, y) | 0 \leq x \leq X,\ 0 \leq y \leq Y\}$ be the domain of 2D points. Let ϕ denote a $n_x \times n_y$ mesh of control points with uniform spacing δ. Let ϕ_{ij} be the value of ij-th control point located at (i , j). The FFD f can be written as:

$$f(x, y) = \sum_{m=0}^{3} \sum_{l=0}^{3} B_l(s) B_m(t) \phi_{i+l, j+m}$$

where, $i = \lfloor x/n_x \rfloor - 1, j = \lfloor y/n_y \rfloor - 1, s = x/n_x - \lfloor x/n_x \rfloor, t = y/n_y - \lfloor y/n_y \rfloor$. B_l and B_m are uniform cubic B-spline basis function defined as:

$$B_0(s) = (1 - s)^3/6$$
$$B_1(s) = (3s^3 - 6s^2 + 4)^3/6$$
$$B_2(s) = (-3s^3 - 3s^2 + 3s + 1)/6$$
$$B_3(s) = (s)^3/6$$

They weigh the contribution of each control point to f(x, y) based on its distance to (x, y). The problem of deriving function f is reduced to solving for the control points in ϕ. The control points in ϕ behave as parameters for transformation. The degree of non-rigid deformation depends highly on the size of control points. Dense mesh can increase number of degrees of freedom, hence providing more flexibility and consequently an increase in computational complexity. In order to achieve the tradeoff between degree of freedom and computational complexity, we use a hierarchical multiresolution [5] approach, in which the resolution of the control mesh is increased, along with the resolution of image in an iterative loop. Consider a hierarchy of control mesh $\phi_0, \phi_1, \ldots, \phi_h$, overlaid on domain Ω. For simplicity, we will assume decreasing space as we move from ϕ_s to ϕ_{s+1}. Similar to above, we will have FFD $f_s(x, y)$ for each control mesh. Their sum defines the overall transformation model.

$$f(x, y) = \sum_{s=1}^{h} f_s(x, y)$$

Calculation of FFD for each control lattice introduces a significant overhead. To avoid this overhead, B-spline refinement can be applied hierarchically to control mesh. This can be achieved by B-spline subdivision algorithm. In this case, the control point mesh at level s is generated by using the mesh control points from level s-1. More details can be found in [4]. To achieve correspondence between two images acquired at different time points, we have used a similarity criterion based on sum of squared difference (SSD):

$$SSD = (1/n) \sqrt{\sum (I(t_0) - T(I(t)))^2}$$

E. Quantification of changes in vascular morphology

Blood vessel growth was quantified by recording the temporal occurrence of differences in pixel intensities along registered vascular structures. Registration is performed on pair of consecutive images (I_t, I_{t+1}). I_t is warped to I_{t+1} to give I_{reg_t}. Measuring the difference (pixel changed) between I_{t+1} and I_{reg_t} provides a standard for change quantification. This protocol is shown in figure 3, where δ_t is the change in number of pixels at time t.

$$\delta_t = I_{t+1} - I_{reg_t}$$

Figure 4 shows an example of two MIP images acquired at consecutive time points and the pixel change measured after registration. The change measured over the entire imaging cycle can be characterized by the function $f(\delta_t)$ given by:

$$f(\delta_t) = \{\delta_t\}_{t=1}^{m}$$

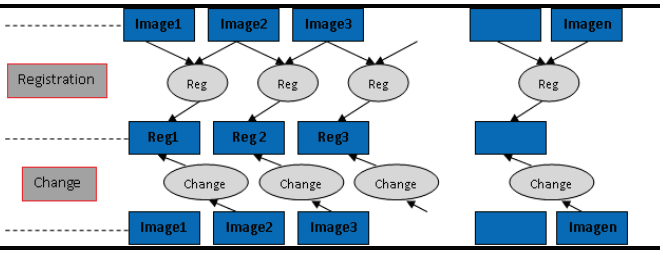

Fig 3. For a given sequence of images, image i is registered to (i +1). Measuring the difference between registered images i and (i + 1), provides the change in number of pixels.

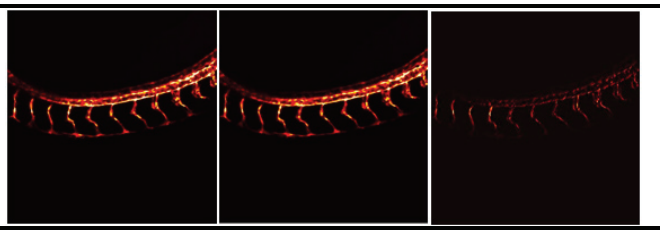

Fig 4. (a) MIP of z-stack acquired at time t, (b) registered MIP of z-stack at time t+1 (c) difference between registered and original MIP. (These images have been modified for visualization by histogram stretching converting the colormap).

III. EXPERIMENTS AND RESULTS

The above computational framework was applied to quantify vascular changes in both toxin treated and untreated zebrafish embryos. A uniform B-splines control grid with spacing [20, 20], and 3 grid refinement levels were used. Totally, 7 embryos (5 untreated and 2 treated) were analyzed.

Vascular growth was computed using method described in section II. Figure 5 shows the dynamics of blood vessel

growth in terms of average pixel change for untreated and arsenic treated embryos. As seen in the figure, although the overall rate of growth is constant for both treated and untreated embryos, the growth rate for untreated embryos is ~5 times higher.

Figure 6 shows the dynamics of blood vessel growth in terms of average pixel change for each of the seven embryos analyzed. Pixel change measured in untreated fish is represented by uexposed1 - uexposed5 and exposed1 - exposed2 shows pixel change measured for arsenic exposed embryos.

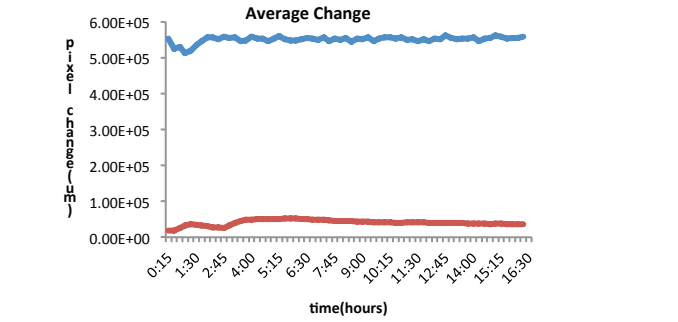

Fig 5. Blue curve shows average change in number of pixels over all the unexposed embryos whereas red curve shows average pixel change for arsenic treated embryo.

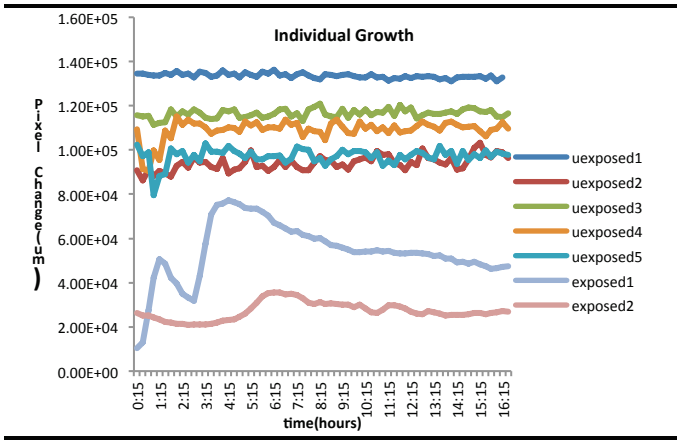

Fig 6. uexposed1 – uexposed5 represents change in number of pixels for unexposed embryos growth, whereas exposed1 and exposed2 represents change in number of pixels for arsenic treated embryos.

IV. CONCLUSION

We show here that toxic effects on blood vessel change can be measured and quantified using method described in this paper. This method can be further applied to generate screening methods for potential toxic environmental pollutants. Roughly 80,000 industrial chemicals are registered on the US market, and very few of them have been screened for vascular disrupting properties. Thus, development of high throughput screening models that generates quantitative data for this biological endpoint is a very important step to identify chemical health threats.

REFERENCES

[1] J. Folkman, "Angiogenesis in cancer, vascular, rheumatoid and other disease", Nature *Med*., vol. 1, 1995, pp.27–31.

[2] K. Dooley and L.I. Zon, "Zebrafish: a model system for the study of human disease", *Curr Opin Genet Dev.,* vol. 10, June 2000, pp. 252–256.

[3] L.I. Zon and R.T. Peterson, "In vivo drug discovery in the zebrafish ", *Nat Rev Drug Discov.,* vol. 4, 2005, pp. 35–44.

[4] D. R. Forsey and R. H. Bartels, "Hierarchical B-spline refinement", *ACM Trans. Comput. Graph*, vol. 22, no. 4, 1988, pp. 205–212.

[5] S. Lee, G. Wolberg, and S. Y. Shin, "Scattered data interpolation with multilevel B-spline ", *IEEE Trans.Visualization Comput. Graph.,* vol.3, July 1997, pp. 228–244.

[6] P. Carmeliet, V. Ferreira, G. Breier, S. Pollefeyt, L. Kieckens, M. Gertsenstein, M. Fahrig, A. Vandenhoeck, K. Harpal, C. Eberhardt, C. Declercq, J. Pawling, L. Moons, D. Collen,W. Risau, A. Nagy, " Abnormal blood vessel development and lethality in embryos lacking a single VEGF allele", *Nature 380*, 1996, pp. 35–439.

[7] N. Ferrara, K. Carver-Moore, H. Chen, M. Dowd, L. Lu, K.S. O'Shea, L. Powell-Braxton, K.J. Hillan, M.W. Moore, "Heterozygous embryonic lethality induced by targeted inactivation of the VEGF gene", *Nature 380*, 1996, pp. 439–442.

[8] F. Shalaby, J. Rossant, T.P. Yamaguchi, M. Gertsenstein, X.F. Wu, M.L. Breitman, A.C. Schuh, "Failure of blood-island formation and vasculogenesis in Flk-1-deficient mice", *Nature 376*, 1995, pp. 62–66.

[9] F. Shalaby, J. Ho,W.L. Stanford, K.D. Fischer, A.C. Schuh, L. Schwartz, A. Bernstein, J. Rossant, "A requirement for Flk1 in primitive and definitive hematopoiesis and vasculogenesis", *Cell 89*, 1997, pp. 981–990.

[10] M. Bro-Nielsen, C. Gramkow, S. Kreiborg. "Non-Rigid Image Registration Using Bone Growth Model", *CVRMed-MRCAS*, March 1997, pp. 3-12.

[11] AS. Andrew, JL. Burgess, MM. Meza, E. Demidenko, MG. Waugh, W. Joshua, Karagas, R. Margaret, "Arsenic Exposure Is Associated with Decreased DNA Repair in Vitro and in Individuals Exposed to Drinking Water Arsenic", *Environ Health Perspect*, vol. 114, no. 8, 2006.

[12] Shugene Lynn, Hsien-Tsung Lai, Jia-Ran Gurr, K-YJan, "Arsenite retards DNA break rejoining by inhibiting DNA ligation", *Mutagenesis*, vol .12, no. 5, 1997, pp. 353-358.

[13] Peter J. Kostelec and Senthil Periaswamy, "Image Registration for MRI", *Modern Signal Processing*, vol. 46, 2003.

[14] M. Betke, H. Hong, and J. P. Ko, "Automatic 3D registration of lung surfaces in computed tomography scans", *Fourth International Conference on Medical Image Computing and Computer-Assisted Intervention*, October 2001, pp. 725–733.

[15] M. Westerfield, "The Zebrafish Book: A Guide for the Laboratory Use of Zebrafish (Danio rerio)", *4th ed. University of Oregon Press*, USA, 2000.

[16] Shuk Han Cheng, Po Kwok Chan, Rudolf Shiu Sun Wu, "The use of microangiography in detecting aberrant vasculature in zebrafish embryos exposed to cadmium", *Aquatic Toxicology*, vol. 52, no. 1, 2001, pp. 61-71.

[17] PK. Chan, SH. Cheng, "Fractal analysis of vascular complexity in cadmium-treated zebrafish embryos", *Aquatic Toxicology*, vol. 63, 2003, pp.83–87.

[18] Cross et al., 2003 L.M. Cross, M.A. Cook, S. Lin, J.N. Chen and A.L. Rubinstein. "Rapid analysis of angiogenesis drugs in a live fluorescent zebrafish assay", *Arterioscler. Thromb. Vasc. Biol.,* vol. 23, 2003, pp. 911–912.